Journal Name

RSCPublishing

ARTICLE

Organic semiconducting layers fabricated by self-metered slot-die coating for solution-processable organic light-emitting devices

Cite this: DOI: 10.1039/x0xx00000x

Received 00th January 2014,
Accepted 00th January 2014

DOI: 10.1039/x0xx00000x

www.rsc.org/

Byoungchoo Park*, O Eun Kwon, Soo Hong Yun, Hong Goo Jeon and Yoon Ho Huh

We present the results of a study of flat, uniform, and stripe-patternable organic semiconducting layers produced by a slot-die coating method using a self-metered coating mode with blended solutions for the fabrication of bright, efficient, and large-area organic light emitting devices (OLEDs). It is shown that the self-metered slot-die coating process can produce high quality, homogeneous, and stripe-patterned thin films using the downstream meniscus of a blended solution, which can be controlled by adjusting the coating parameters of the capillary number of the coating solution by varying the gap height and coating speed. It is shown that very bright and efficient OLEDs (peak brightness ~50,000 cd m^{-2} with maximum efficiencies of ~29 cd A^{-1} and ~14 lm W^{-1}) were successfully demonstrated by manipulating the slot-die coated hole-injecting and electroluminescent layers that contained phosphorescent Ir complex. In view of these results, we believe that the fabrication of organic semiconducting layers using the self-metered slot-die coating process is a promising new technique for high-throughput manufacturing such as via the roll-to-roll process.

Introduction

Following the pioneering studies of the first organic light emitting devices (OLEDs) made of polymeric and/or small molecular materials, a number of important studies have been undertaken on the development of the organic materials and device structures needed to realise economical, lightweight, flexible, and large–area electronic devices.[1-14] The major scientific and technological issues in the performance of organic devices pertain to their efficiency, stability, and simplicity in terms of their fabrication. One particular example relates to the internal quantum efficiency of OLEDs, which has seen significant improvement of late, reaching nearly 100% following the incorporation of phosphorescent emitters into the electroluminescent (EL) layer. Strong spin-orbit coupling now leads to rapid intersystem crossing and a radiative transition from triplet states to a ground state, thereby enabling enhanced EL emissions.[3-6] Using the phosphorescent Ir complex, electrophosphorescent OLEDs (PHOLEDs) with a high peak luminescence of up to ca. 50,000-100,000 cd m^{-2} have now been demonstrated.[3-6] At the same time, relatively little progress has been made with respect to achieving reliable and simple fabrication, although it is clear that the establishment of a flat and uniform organic layer covering a large area is particularly important for achieving efficient and reliable device performance in organic electronics. In general terms, in the fabrication of OLEDs, organic layers have typically been prepared either by physical vapour deposition or by a wet solution-coating process.[1-14] To date, vapour-deposited organic layers of small molecular materials have shown the best performances, although the vapour-deposition process is complex and expensive. Solution-processed devices made of polymeric or small molecular materials are therefore of some interest, because they allow simple production techniques to be applied with a non-vacuum process.[7-14] Spin-coating has been the most popular method of forming organic layers in such solution-processed devices. Nevertheless, this convenient method has several disadvantages; for example, the spinning motion causes the build-up of stress, there is poor uniformity at the edges of large areas, and a large amount of solution is wasted. These factors make spin-coating unsuitable for large active areas. One alternative means of achieving the same outcome is via the use of printing, such as screen printing,[9] ink-jet printing,[10] or blade coating.[11] Using these printing or coating techniques, organic layers can be formed on substrates in a controlled fashion. One other method that could be used to deposit solution is the use of wire-bar coating.[13] Organic film made using wire-bar coating is generally more homogeneous than that made by doctor-blade coating.[13] Recent reports have shown that using the printing and/or coating techniques described above, efficient devices can be obtained; in particular, organic field effect transistors (OFETs).[15,16] However, there are very few studies or reports of such solution-coating techniques, and fundamental information on the coating process used to produce flat, uniform, and homogeneous films for fabricating highly bright, efficient, and large-area OLEDs is somewhat limited.[12,13]

In the continued search for a more suitable method, the all-solution-based fabrication of a light-emitting electrochemical cell (LEC) was recently demonstrated using slot-die coating.[14]

This technique belongs in the category of pre-metered coating methods, because the thickness of the coated film can be predetermined.[17-19] For this reason it is considered to be a powerful and versatile method for products requiring advanced coatings, including patch coating for large pieces of glass,[17] tensioned-web slot coating for thin optical films,[18] and stripe coating for colour filters.[19] However, in one set of tests the reported brightness and efficiency of the resulting LEC were lower (about 150 cd m^{-2} and 0.6 cd A^{-1}, respectively) than those (about 70,000 cd m^{-2} and 9 cd A^{-1}, respectively) of conventional OLEDs fabricated using spin-coated layers.[11] Moreover, there is very limited scientific understanding of the coating operation associated with coating types in film fabrication and of the device performance of OLEDs fabricated.[20] There is therefore a pressing need to consider alternative methods of fabricating solution-processable organic semiconducting layers, in the search for brighter and more efficient OLEDs that are superior or at least comparable to spin-coated devices in terms of performance, without the less undesirable characteristics of spin-coated devices.

We herein advance a unique slot-die coating method for fabricating organic semiconducting layers for bright and efficient OLEDs. In a significant development of the conventional pre-metered slot-die coating method, we present for the first time a self-metered slot-die coating method for fabricating organic layers for the production of highly bright and efficient OLEDs. The advantage of self-metered coating is that the coating thickness can be controlled easily and precisely by external parameters such as the viscosity, the surface tension of the coating solution, and the coating speed, in contrast to more typical pre-metered slot-die coating methods. We recently showed the effectiveness of a similar coating method for highly efficient OLEDs fabricated using a solution-coating process for horizontal-dip coating (H-dip coating).[12] In the present study we provide systematic studies of the slot-die coating operations in the self-metered coating region and describe solution-processed OLEDs with a high efficiency and performance, using self-metered slot-die coated layers.

Self-metered slot-die coating process

A photographic image and schematic diagram for the slot-die coating process studied here are shown in Fig. 1(a). As shown in the figure, a slot-die head is hung at a specific height (h_0) above a substrate applied to a carrying stage that transports it horizontally. The slot-die coating process used in this study proceeds according to the following steps. (1) The substrate is attached to the carrying stage and the slot-die head is placed at the front edge of the substrate. An organic (or inorganic) molecular solution is then pumped from a reservoir through a filter and into the slot-die head. The slot-die head delivers the coating solution through a slot-nozzle into the empty space (gap region) between the slot-nozzle (via a shim-mask) and the substrate by capillary action, so that a uniform downstream meniscus of coating solution is formed on the substrate, attracted by the surface tension to the slot-die head. (2) Next, the substrate is transported horizontally at a given speed U while the shape of the downstream meniscus is maintained. A thin, stripe-patterned solution layer of the downstream meniscus is then spread on the substrate, with the coating solution being supplied into the gap at an appropriate pumping rate. (3) The wet film coated on the substrate is then dried; a heater may be used to assist the evaporation of the residual solvent. Using this process, it is possible to obtain a substrate

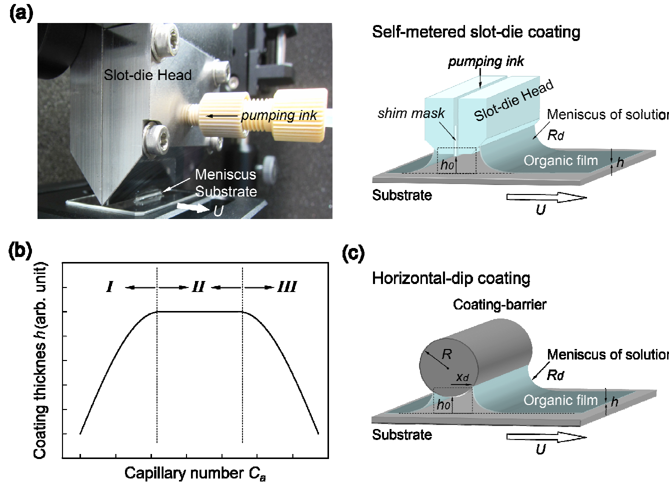

Fig. 1 (a) Photograph (left) and its schematic illustration (right) of the self-metered slot-die coating process studied, showing the gap height h_0 and coating speed U. (b) Three regions of dimensionless minimum wet thickness h as a function of capillary number Ca of the coating solution. (c) A comparative Horizontal-dip coating process.

coated with a stripe-patterned solid film of uniform thickness. It can be seen that the stripe widths of the coated films can be controlled by the widths and shape of the shim mask. The detailed dimensions of the slot-die head and ranges of experimental parameters used here are listed in the Experimental Methods section.

Previous studies of slot-die coating processes[19,21] have indicated that there exist three possible regions of minimum wet thickness in coating flows when considering the coating thickness h vs. capillary number $Ca=(\mu U/\sigma)$ of the coating solution, where μ and σ represent the viscosity and surface tension of the coating solution, respectively, and U is the carrying (coating) speed, as shown in Fig. 1(b). Defect-free coating is possible only when the coating operation is performed above this curve. In Region I ($Ca \ll 1$), the coating thickness h increases with increasing Ca. This behaviour is consistent with "dip coating" as predicted theoretically by Ruschak.[22] Region II describes the case where h is independent of Ca,[23] while in Region III a further increase in Ca results in a reduction in coating thickness h, as in a liquid jet impinging on a moving substrate. In the present study we investigated self-metered coating, which operates in Region I, in order to achieve fine control of the thickness of the coated layer by adjusting the capillary number Ca (coating speed U).

It is noteworthy that the self-metered slot-die coating technique used herein, using the meniscus of the solution, is similar to dip coating or H-dip coating (Fig. 1(c)),[12] in that substrates are immersed in coating solution and wet layers are then formed by withdrawing the substrates vertically or horizontally through the menisci of the coating solutions, respectively. Similar to the H-dip coating method, in the proposed slot-die coating process the wet film is formed via the horizontal withdrawal of the substrate. The film thickness achieved by the solution-coating process in Region I can be explained by the description of the associated drag-out problem, as suggested by Landau and Levich.[24] In the Landau-Levich problem the deposited thin film is "self-metered", so that the thickness is determined by the parameters of the problem. Based on their description, for a coating solution with a low capillary number ($C_a \ll 1$), a useful relationship may be obtained between the thickness of the film emerging from a coating bead and the radius of the associated downstream meniscus R_d and the capillary number C_a:[12,24]

$$h = k\, C_a^{2/3} \cdot R_d = k\left(\frac{\mu U}{\sigma}\right)^{2/3} \cdot R_d \,, \qquad (1)$$

where k is a constant of proportionality. It is noteworthy that the thickness of the self-metered slot-die coated film increases with the coating speed. This is one of the critical ways in which the self-metered coating mode of Region *I* differs from the conventional coating mode of Region *II*. In our self-metered coating process, precise control of the thickness is possible, allowing the production of extremely thin films.

Experimental

Fabrication of OLEDs. An indium tin oxide (ITO) layer (80 nm, 30 ohm square^{-1}) on a glass substrate was used as a transparent anode. The ITO substrate was ultrasonically cleaned and then dried in sequence, followed by ultra-violet ozone cleaning for 15 min. Then, a blended poly(3,4-ethylenedioxythiophene): poly(styrene sulfonate) (PEDOT:PSS) solution was used for slot-die coating of the ITO layer to form a hole-injecting layer (HIL). The PEDOT:PSS solution used was a mixture of 1 % PEDOT:PSS solution (CLEVIOS™ P VP AI 4083, H.C. Starck) and isopropyl alcohol with a weight ratio of 1 : 3. In order to maintain the shape of the downstream meniscus during slot-die coating, the PEDOT:PSS dispersion was supplied into the gap space using a syringe pump (Pump Systems Inc. NE-1000) at an appropriate injection rate (~1.5 µl s^{-1}). The viscosity of the mixed PEDOT:PSS solution, measured by viscometer (RVDVII+, Brookfield Inc.), was about 11.6 cp. A blended EL solution was used for the slot-die coating of the ITO layer, precoated with the PEDOT:PSS HIL. For the blended EL solution, we used N,N'-diphenyl-N,N'-bis(3-methylphenyl)-1,1'biphenyl-4,4'-diamine (TPD), 2-(4-Biphenylyl)-5-(4-tert-butylphenyl)-1,3,4-oxadiazole (Bu-PBD), tris(2- Phenylpyridinato) iridium ($Ir(ppy)_3$), and poly(vinylcarbazole) (PVK) introduced without further purification

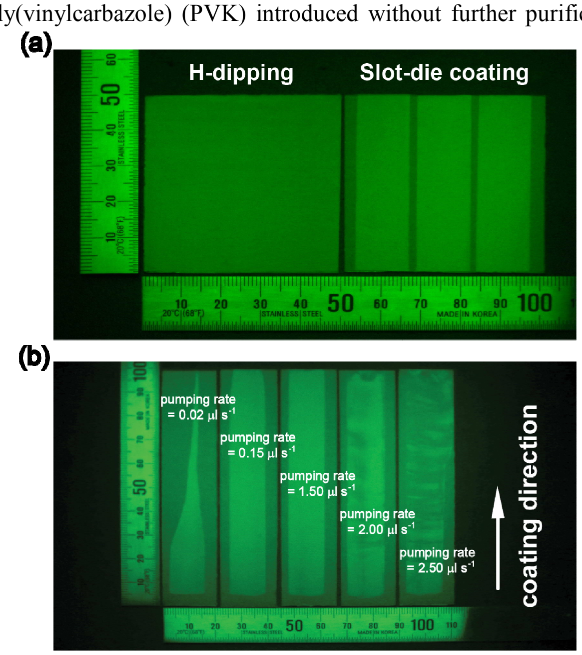

Fig. 2 (a) Photographs of H-dip (left) and self-metered slot-die coated (right) EL films on 5 × 5 cm^2 substrates under monochromatic light (546.1 nm). (b) Photographs of the self-metered slot-die coated strips of EL films for five different pumping rates of coating solution.

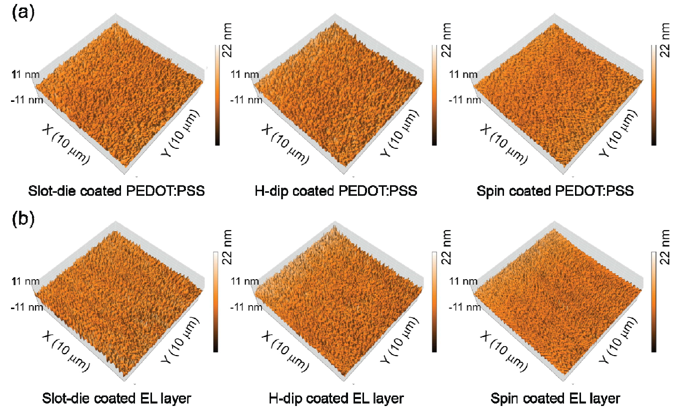

Fig. 3 AFM topography images of the PEDOT:PSS HIL (a) and EL (b) layers on glass substrates using the slot-die (left), H-dip (middle), and spin (right) coating methods.

into mixed solvents of 1,2-dichloroethane and chloroform (3:1).[12] The viscosity of the EL solution was about ~1.0 cp. The apparatus used for slot-die coating had a maximum work space of 10 × 10 cm^2 with a commercial 12-mm-wide slot-die head (FOM Technologies, shim-mask width = 10.0 mm). The height of the gap h_0 was adjusted vertically using two micrometer positioners, and the carrying speed U was adjusted by a computer-controlled translation stage (SGSP26-200, Sigma Koki Co., Ltd). After a meniscus had formed on the substrate, the substrate was transported horizontally, so that the slot-die head spread the solution on the transporting substrate. The transporting speed U was 1.5 cm s^{-1}. It took 3.3 s to coat a complete film on a substrate over an area of 1.0 × 5.0 cm^2. The slot-die coated PEDOT:PSS HIL was then dried using a heating plate at 110°C for 20 min, in order to remove the remaining solvents. Sequentially, 2 nm Cs_2CO_3 and 60 nm of Al were evaporated on the EL layer via thermal deposition (0.5 nm s^{-1}) at a base pressure below 2.7 × 10^{-4} Pa. Thus, the OLED in our study had a device configuration of Glass/ ITO/ PEDOT:PSS/ EL layer/ Cs_2CO_3/ Al. For comparison, reference and comparative OLEDs were fabricated by spin and H-dip coating methods, respectively, using the blend solutions.

Film and device characterization. A Chroma Meter CS-200 (Konica Minolta Sensing, INC.), a spectrometer (Ocean's Optics), and a source meter (Keithley 2400) were used to measure the EL characteristics. Characterisation of the device was carried out at room temperature under ambient conditions, without encapsulation. The impedance spectroscopy (IS) measurements for the fabricated devices were performed using an HP 4192A at frequencies ranging from 20 Hz to 13 MHz, with a 100 mV perturbation oscillation signal to maintain the linearity of the response. All IS measurements were performed in the dark with different bias voltages.

Results and discussion

Slot-die coated organic layers

To begin with, we observed optical interference images of the slot-die and H-dip coated organic EL layers (80 nm thick) on 5 × 5 cm^2 glass substrates with the naked eye using a monochromatic Hg light with a wavelength of 546.1 nm, as shown in Fig. 2(a). It may be seen from the figure that the slot-die coated stripe-patterned films (line width = 12 mm, line separation = 3 mm) are very smooth and uniform, similar to the H-dip coated film. Variations in the thickness of the slot-die coated film were observed only at the very rear of the stripe-

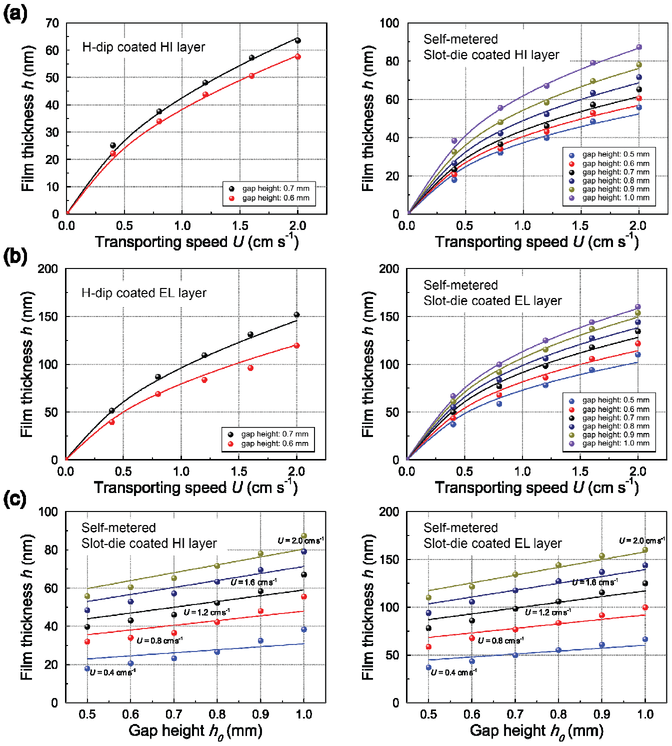

Fig. 4 Coated film thickness data of the PEDOT:PSS (a) and EL (b) layers as a function of coating speed U for different gap heights h_0 of the H-dip (left) and self-metered slot-die (right) coating processes. (c) Film thickness data of the layers as a function of gap height h_0 for several coating speeds of the self-metered slot-die coating process. The solid curves show the theoretical predictions of the Landau & Levich equation.

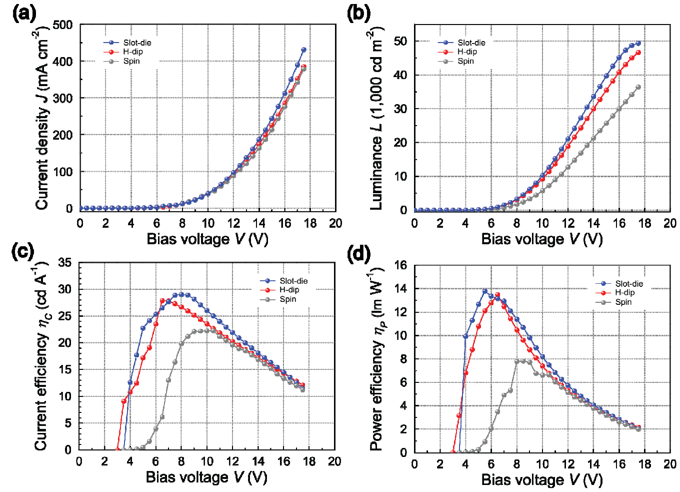

Fig. 5 Current density-voltage (J-V) (a) and luminance-voltage (L-V) (b) characteristics of the OLEDs made by the slot-die, H-dip, and spin-coating processes. Current efficiency-voltage (η_c-V) (c) and power efficiency-voltage (η_p -V) (d) characteristics of the OLEDs studied.

patterned edges of the coated films, which may be due to the Bernoulli or coffee-ring effect.[25] In order to produce a fully smooth slot-die coated film, the speed of coating and the viscosity, as well as the injection pumping rate of the coating solutions, must be adjusted to suit. For the pumping rate, when the rate is lower than the optimum rate (~ 1.5 μl s^{-1}), the fabricated film tends to be thin and inhomogeneous, with a narrowing width of coating area due to the reduction of meniscus volume, while if the rate is too high (>1.5 μl s^{-1}), the film quality tends to be inhomogeneous due to significant variations in the form of the meniscus of the coating beads during the coating process (Fig. 2(b)). The appropriate determination of optimum pumping rate is therefore important in order to obtain homogenous and continuous films over a large area in the self-metered slot-die coating used.

For the further investigation of the surface morphologies of the fabricated films, the variation in the surface roughness of the fabricated films was monitored using an atomic force microscope (AFM, Nanosurf easyscan2 AFM, Nanosurf AG Switzerland Inc.) (Fig. 3). This revealed the topography to be fairly uniform; the root mean square (rms) roughness of the slot-die coated PEDOT:PSS HIL film was only *ca*. 1.1 nm, which is comparable to those (*ca*. 0.8~0.9 nm) of H-dip and spin-coated films. Moreover, the rms roughness of the slot-die coated EL layer was also only *ca*. 1.1 nm, which is also comparable to those (*ca*. 1.0 nm) of H-dip and spin-coated layers. It is thus possible to achieve reliable and uniform film thicknesses of both the HIL and the EL layers using self-metered slot-die-coating, even on a large-area substrate, because of the effective control of the undesirable flow at the top surface of the wet-film via the surface tension of the solution by the coating head, similar to the H-dip-coating method.

We next investigated the dependence of film thickness h of the self-metered slot-die coated PEDOT:PSS HIL and EL layers on the coating speed U and the gap height h_0. The measured results are shown in Fig. 4. As shown in Figs. 4(a) and (b), the dependence of the film thickness of both the self-metered slot-die coated HIL and the EL layers on the coating speed and the gap height shows nearly the same dependence as the H-dip coated layers: the thicknesses of both the HIL and the EL layers increase continuously as the coating speed U increases in the observed region for a given gap height. Moreover, when h_0 is increased, the thickness of the self-metered slot-die coated HIL and EL layers also increase for a given coating speed U. As also shown in Fig. 4(c), it is clearly confirmed that the thickness of the HIL and EL layers increase continuously when h_0 is increased. All these results can be explained in terms of the associated drag-out problem, as per Equation (1). The curve-fitted results using Equation (1) are also shown in the figures (solid curves). The observed data show good agreement with the theoretical values predicted by the equation, indicating that the thickness of the slot-die coated films can also be controlled with some precision by adjusting the gap height h_0 and coating speed U. It is therefore evident that the thicknesses of the slot-die coated layers show almost the same trends as those of the H-dip coated layers.

Structure and fabrication of the OLEDs with the slot-die coated layers

We next investigated the device performance of the sample OLED produced by the slot-die coating process. Using the above information on layer thickness, we prepared slot-die coated OLEDs with device configuration Glass/ ITO anode/ PEDOT:PSS HIL/ EL layer/ Cs_2CO_3 electron injection layer (EIL)/ Al cathode. Both the PEDOT:PSS HIL and the organic EL layers were subsequently coated on an ITO-coated glass substrate using the self-metered slot-die coating process. The thicknesses of the PEDOT:PSS HIL and EL layer were adjusted to about 40 nm and 80 nm, respectively. Figure 5 shows the observed current density-luminance-voltage (*J-L-V*) characteristics of the sample OLED. The slope of the *J-L-V* curve between 0 V and 18 V shows the excellent diodic behaviour of the sample OLED and thus illustrates the good coverage of the slot-die coated HIL and EL layers. It is clear from the *J-L-V* characteristics that both the charge injection and turn-on voltage are below 3.4 V, with sharp increases in the curves. The operating voltage is about 6.7 V for a brightness of 1,000 cd m^{-2}, and 9.9 V for 10,000 cd m^{-2}; the luminescence reached *ca*. 50,000 cd m^{-2} (at 17.5 V). It is noteworthy that the brightness of 50,000 cd m^{-2} is among the highest value reported to date for OLEDs made using a slot-die coating process. To confirm the high performance of the sample devices, we deduced the efficiency of the devices studied, as shown in Fig. 5(c). For the slot-die coated sample OLED, a maximum current efficiency η_c of 29.0 cd A^{-1} was obtained at 3,300 cd m^{-2} (at 8.0 V). We also obtained the power efficiency η_p of the sample device, which reached a maximum of 13.8 lm W^{-1} (at 5.5 V). For the comparative H-dip coated device, all the EL characteristics are similar to those of the slot-die coated sample device; the turn-on voltage is below 3.4 V and the operating voltage is about 6.7 V for a brightness of 1,000 cd m^{-2}, and 10.3 V for 10,000 cd m^{-2}; the maximum luminescence reached *ca*. 47,000 cd m^{-2} (at 17.5 V) with a maximum η_c = 27.9 cd A^{-1} (at 6.5 V, 880 cd m^{-2}) and maximum η_p = 13.5 lm W^{-1} (at 6.5 V). For the reference spin-coated device, the turn-on voltage was *ca*. 3.4 V and the operating voltage was about 7.3 V for a brightness of 1,000 cd m^{-2}, and 11.3 V for 10,000 cd m^{-2}; the maximum luminescence reached *ca*. 36,000 cd m^{-2} (at 17.5 V) with a maximum η_c = 22.2 cd A^{-1} (at 10.0 V, ~5,800 cd m^{-2}) and maximum η_p = 7.8 lm W^{-1} (at 8.5 V, ~2,500 cd m^{-2}), all of which values are somewhat lower than those of the sample and comparative devices. Our results therefore clearly show that the self-metered slot-die coating process can produce efficient and bright HIL and EL layers.

Impedance characteristics of the OLEDs with the slot-die coated layers

Next, in order to investigate the charge carrier injecting and transporting properties of the self-metered slot-die coated layers in the sample OLED, we observed the impedance characteristics of the devices using IS. This powerful method is commonly used to characterise the electrical properties of materials and their interfaces.[26,27] Figure 6(a) shows representative examples of the plots of the real (Re(Z)) and imaginary (-Im(Z)) parts of the complex impedance (*Z*) (Cole-Cole plots) at frequencies *f* between 20 Hz and 13 MHz for the OLEDs studied at bias voltages of 3.5 V and 5.5 V. In these plots, the implicit variation is in the frequency, which increases from right to left. It is clear that the impedance spectra resemble those of a single-layer device, giving a single semicircle in the Cole–Cole plots, with the size of the semicircle decreasing abruptly with increasing bias voltage. The maximum Re(*Z*) value represents the summation of the series resistance and the parallel resistance with the capacitor. Thus the equivalent circuit for the OLED devices studied can be considered to be a single parallel resistor R_P and capacitor C_P network with a series resistance R_S, as shown in the inset of the figure.[28] The equivalent circuit analysis using the fitting parameters R_S, R_P, and C_P for the sample OLED device at different bias voltages yields the variations in the fitting parameters at different bias voltages. The estimated value of R_S is about 35.7 ohm and varies slightly with bias voltage (± 0.22) (Fig. 6(b)), which may originate from the contact at the electrode interface. The bulk capacitor C_P of 2.55 nF is also almost independent of the bias, while the bulk resistance R_P decreases rapidly with increasing bias voltage (Fig. 6(b)). These behaviours indicate that as the bias is increased, an ever greater number of charge carriers is injected into the device, resulting in a decrease in the dielectric relaxation time τs, and decreasing the bulk resistance R_P.[29] Here, the relaxation frequency f_r satisfies the relationship $2\pi f_r = \tau^{-1}$; for example, at a bias voltage of 3.5 V, the sample device shows an f_r value of approximately 0.10 kHz, while f_r for the device is approximately 1.74 kHz at a bias voltage of 5.5 V.

Similarly, the H-dip coated comparative devices show an R_S of 36.8 ohm and a C_P of 2.61 nF, which are similar to those of the sample device. Moreover, at a bias voltage of 3.5 V, the comparative device shows f_r values of approximately 0.33 kHz,

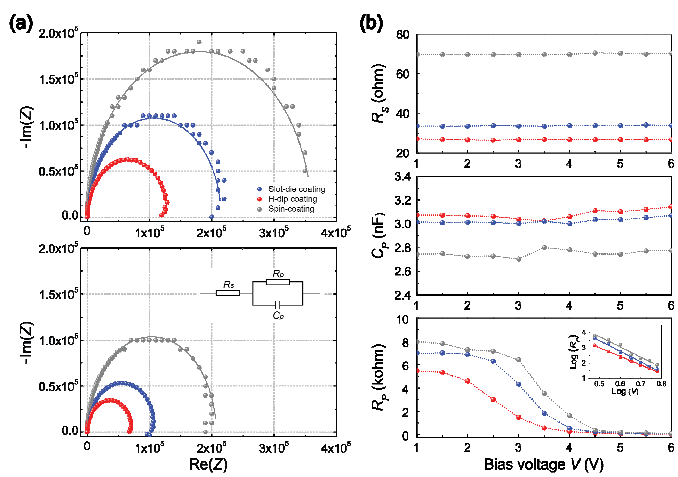

Fig. 6 (a) Cole–Cole plots of the real and imaginary parts of the complex impedance (*Z*) for the OLEDs fabricated by slot-die, H-dip, and spin-coating methods at bias voltages of 3.5 V (upper) and 5.5 V (lower). The inset shows an equivalent circuit to describe the impedance spectroscopy. The solid curves are the simulated results according to the equivalent circuit. (b) The variation of the obtained series resistance R_S (upper), parallel capacitance C_P (middle), and parallel resistance R_P (lower) with bias voltage for the OLEDs studied. The inset shows the variations of log(R_P) with log(V).

while f_r for the devices is approximately 2.09 kHz at a bias voltage of 5.5 V, clearly indicating that f_r for the comparative device is similar to that of the sample device. These IS results clearly indicate that carrier (hole) injection in the slot-die coated sample device is as efficient (high relaxation frequency)[30] as it is in the H-dip coated comparative device. In contrast to the comparative device, the IS behaviour of the spin-coated reference OLED differs significantly from that of the slot-die coated sample OLED; the spin-coated device shows a C_P of 2.35 nF and an R_S of 80.7 ohm, which are very different from the sample and comparative devices. It is also noteworthy that as shown in the figure, the R_P value of the spin-coated OLED is higher than those for the slot-die coated sample and the H-dip coated comparative devices, implying that the spin-coated layer may contain more trap sites than the others due to structural impurities or defects.[31,32] Moreover, the spin-coated reference device exhibits an f_r value of 0.03 kHz at a bias voltage of 3.5 V and an f_r value of approximately 1.20 kHz at a bias voltage of 5.5 V. These results show that the values of f_r for the sample device are higher than those for the spin-coated reference device.

To gain a better understanding of the current flows in the OLED devices, we also investigated the dependence of R_P on the voltage V. The plots of log(R_P) vs log(V) for the OLEDs studied are shown in the inset of Fig. 6(b). It is clear that log(R_P) for the OLEDs studied is linearly dependent on log(V). From space-charge-limited current (SCLC) theory, the voltage-dependent current J for one-carrier dominated transport, hole in this case, is given by $J \propto V^{m+1}$, and thus the slope of log(R_P) vs log(V) gives information on the exponent m.[32-34] For the OLEDs studied, we obtained m values of about 6.3 for the slot-die coated sample in the voltage range of $3\text{V} < V < 6$ V, which lies between the m values of the spin-coated reference device (m = 7.5) and the comparative H-dip coated device (m = 4.8), implying that the conductance of the holes for the slot-die, H-dip, and spin coated PEDOT:PSS/EL layers follow SCLC theory, with exponential trap distribution ($m > 2$) rather than trap-free SCLC (m = 2).[32-34] The details of the underlying mechanism of the carrier transport needs further investigation, which will be reported elsewhere.

The foregoing IS results clearly show that the charge carrier injecting, transporting, and relaxation properties of the self-metered slot-die coated OLED device are similar to those of the H-dip coated OLED device, but quite different from those of the spin-coated device. By combining our IS results with the performance (J-L-V) data of the OLED devices shown in Fig. 5, it can be seen that slot-die coated layers possess efficient charge-injection and transport properties (high relaxation frequency), which are similar to those of H-dip coated layers and better than those of conventional spin-coated layers. It is therefore clear that an OLED device with slot-die coated layers is a sensible option due to its low series resistance R_S, high relaxation frequency (good charge injection), and high luminance efficiency.

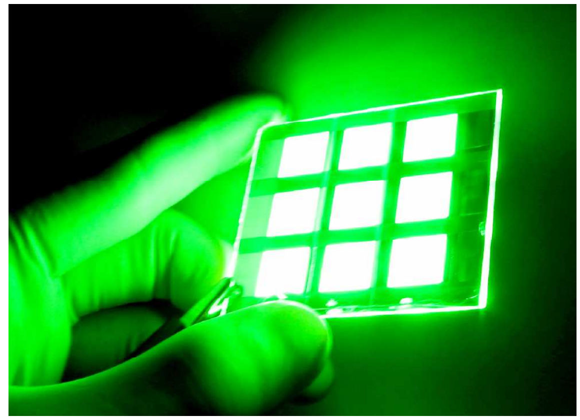

Fig. 7 Photograph of the 3 × 3 OLED pixels (line width = 12 mm, line separation = 3 mm), fabricated using the self-metered slot-die coating method, operating at 10 V on a glass substrate (5 cm × 5 cm).

Fabrication of the 3 × 3 OLED pixels using the self-metered slot-die coating method

Finally, in order to check the ease of processability of large-area and patternable solution-processed OLEDs made using the self-metered slot-die coating method, we fabricated test OLEDs on a 5 × 5 cm^2 ITO-coated glass substrate. A photographic image of the fabricated device is shown in Fig. 7. On a strip-patterned ITO glass substrate, a PEDOT:PSS HIL and an EL layer were deposited using self-metered slot-die coating to produce a green OLED lighting device. The pixel array was 3 × 3 and the pixel size was about 12 × 12 mm^2. As shown in the figure, the OLEDs produced are fairly luminous. The EL spectra, collected from each of the 9 individual pixels on the substrate, were almost identical for each pixel (not shown); the emission peak wavelength was about 510 nm and the full width at half maximum was about 170 nm. The low variation in emission intensity in the different pixels implies a small variation in thickness of the solution-coated layers. Furthermore, this low variation in EL intensity implies the suitability of this method for large-scale fabrication. These results demonstrate that the slot-die coating method allows fabrication to be simple, with easy scaling up to larger sizes at lower cost than for other processes. It also implies that the self-metered slot-die coating process is suitable for fabricating stripe-patterned thin films. We note that the performance of the OLEDs could be further improved by selecting optimal materials, solvents, solution concentrations, viscosities, gap height between the barrier and the substrate, etc.

From the above observations, it is clear that the self-metered slot-die coating process shows considerable promise for the production of flat, uniform, large-area, and stripe-patterned organic semiconducting layers, allowing the realisation of fast processing, low-cost, bright, and efficient OLEDs. Furthermore, the self-metered slot-die coating process used in this study could also be applied to the design of new electrical organic devices such as organic solar cells, transistors, special organic lighting devices, memories, and sensors.

Conclusions

In summary, a simple self-metered slot-die coating process was shown to produce thin organic semiconducting layers for cost-efficient, large-area, and stripe-patternable OLEDs. Our experimental results demonstrate that the self-metered slot-die coating process can allow critical control of the thickness, and produces extremely thin, high quality films at line speeds of the order of a few metres per minute. It was also shown that bright (~ 50,000 cd m^{-2}), efficient (~29 cd A^{-1}), and patterned OLEDs can be produced that perform comparably to OLEDs made using the H-dip-coating process. Moreover, it is also shown that the OLEDs fabricated using self-metered slot-die coating exhibited better injection and transport properties of the charge carriers than conventional spin-coated devices, which could yield deep fundamental insights into the mechanisms of charge carrier injection and transport in solution-processable OLEDs. Thin organic semiconducting layers were successfully applied to a 5 cm × 5 cm glass substrate with a high degree of uniformity using the slot-die coating process by controlling the meniscus of the solution via the gap height and coating speed. These results clearly indicate that the self-metered slot-die coating method has great potential for applications to large-area and patterned OLEDs. This novel process for depositing solution on substrate could be extended to roll-to-roll coating methods, and will provide a solid foundation for extending the fabrication of large-area organic devices to include various advanced types of OLEDs. Using the slot-die coating method reported here together with highly luminous organic materials reported elsewhere could lead to the successful fabrication of highly luminous large-area, and stripe-patternable OLEDs, rendering such devices acceptable in many applications, including lighting, displays, and/or optoelectronic devices.

Acknowledgements

This work was supported by the Basic Science Research Program through a National Research Foundation of Korea (NRF) Grant funded by the Korea Government (MEST) (2010-0029416, 2012R1A2A2A01015654); the Converging Research Center Program through the Ministry of Science, ICT and Future Planning, Korea (2013K000162); the Chungcheong Institute for Regional Program Evaluation Promotion Project of the Korean Ministry of Knowledge Economy (R0001445); and by Kwangwoon University (2014).

Notes and references

Department of Electrophysics, Kwangwoon University, Seoul 139-701, Korea. Fax: 82 2943 3208; Tel: 82 2940 5237; E-mail: bcpark@kw.ac.kr

1 C. W. Tang and S. A. VanSlyke, *Appl. Phys. Lett.,* 1987, **51**, 913.
2 J. H. Burroughes, D. D. C. Bradley, A. R. Brown, R. N. Marks, K. Mackay, R. H. Friend, P. L. Burns and A. B. Holmes, *Nature,* 1990, **347**, 539.
3 M. A. Baldo, D. F. O'Brien, Y. You, A. Shoustikov, S. Sibley, M. E. Thompson and S. R. Forrest, *Nature,* 1998, **395**, 151.
4 M. A. Baldo, S. Lamansky, P. E. Burrows, M. E. Thompson and S. R. Forrest, *Appl. Phys. Lett.,* 1999, **75**, 4.
5 C. Adachi, M. E. Thompson and S. R. Forrest, *IEEE J. Sel. Top. Quantum Electron.,* 2002, **8**, 372.
6 G. He, M. Pfeiffer, K. Leo, M. Hofmann, J. Birnstock, R. Pudzich and J. Salbeck, *Appl. Phys. Lett.,* 2004, **85**, 3911.
7 J. Ouyang, T.-F. Guo, Y. Yang, H. Higuchi, M. Yoshioka and T. Nagatsuka, *Adv. Mater.,* 2002, **14**, 915.
8 F. So, B. Krummacher, M. K. Mathai, D. Poplavskyy, S. A. Choulis and V.-E. Choong, *J. Appl. Phys.,* 2007, **102**, 091101.
9 D. A. Pardo, G. E. Jabbour and N. Peyghambarian, *Adv. Mater.,* 2000, **12**, 1249.
10 B.-J. de Gans, P. C. Duineveld and U. S. Schubert, *Adv. Mater.,* 2004, **16**, 203.
11 S.-R. Tseng, H.-F. Meng, K.-C. Lee and S.-F. Horng, *Appl. Phys. Lett.,* 2008, **93**, 153308.
12 B. Park and M.-Y. Han, *Opt. Express,* 2009, **17**, 21362.
13 T. Koyama, S. Naka and H. Okada, *Jpn. J. Appl. Phys.,* 2012, **51**, 112102.
14 A. Sandström, H. F. Dam, F. C. Krebs and L. Edman, *Nat. Commun.,* 2012, **3**, 1002.
15 C. E. Murphy, L. Yang, S. Ray, L. Yu, S. Knox and N. Stingelin, *J. Appl. Phys.*, 2011, **110**, 093523.
16 D. Khim, H. Han, K.-J. Baeg, J. Kim, S.-W. Kwak, D.-Y. Kim and Y.-Y. Noh, *Adv. Mater.*, 2013, **25**, 4302.
17 *US Pat.,* 4 938 994, 1990.
18 J. Q. Feng, *AIChE J.,* 1998, **44**, 2137.
19 *JP Pat.,* 2003-344642, 2003.
20 T. J. Faircloth, J. G. Innocenzo and C. D. Lang, *SID Symp. Dig. Tech. Papers*, 2008, **39**, 645.
21 Y.-R. Chang, H.-M. Chang, C.-F. Lin, T.-J. Liu and P-Y Wu, *J. Colloid Interface Sci.,* 2007, **308**, 222.
22 K. J. Ruschak, *Chem. Eng. Sci.,* 1976, **31**, 1057.
23 T. Sullivan, S. Middleman and R. Keunings, *AICHE J.,* 1987, **33**, 2047.
24 L. D. Landau and V. G. Levich, *Acta Physicochimica URSS,* 1942, **17**, 42.
25 R. D. Deegan, O. Bakajin, T. F. Dupont, G. Huber, S. R. Nagel and T. A. Witten, *Nature,* 1997, **389**, 827.
26 I. H. Campbell, D. L. Smith and J. P. Ferraris, *Appl. Phys. Lett.,* 1995, **66**, 3030.
27 S. Berleb and W. Brütting, *Phys. Rev. Lett.,* 2002, **89**, 286601.
28 V. Shrotriya and Y. Yang, *J. Appl. Phys.,* 2005, **97**, 054504.
29 C. H. Kim, O. Yaghmazadeh, D. Tondelier, Y. B. Jeong, Y. Bonnassieux and G. Horowitz, *J. Appl. Phys.,* 2011, **109**, 083710.
30 S. Nowy, W. Ren, J. Wagner, J. A. Weber and W. Brütting, *Proc. SPIE,* 2009, **7415**, 74150G.
31 R. Schmechel and H. von Seggern, *Phys. Stat. Sol. C,* 2004, **201**, 1215.
32 M. A. Lampert and P. Mark, in *Current Injection in Solids*, ed., M. A. Lampert and P. Mark, Acardemic Press, New York, 1st edn., 1970.
33 K. C. Kao and W. Hwang, in *Electrical transporting in solids, with particular reference to organic semiconductors*, ed. K. C. Kao and W. Hwang, Academic Press, New York, 1st edn., 1981.
34 M. Pope and C. E. Swenberg, in *Electric processes in organic crystals and polymers*, ed. M. Pope and C. E. Swenberg, Oxford University Press, Oxford., 2nd edn., 1999.

Journal Name RSCPublishing

ARTICLE